Title: The Eyjafjallajökull ash plume - Part I: Physical, chemical and optical characteristics

Author(s): Colin O'Dowd[1], Darius Ceburnis[1], Jurgita Ovadnevaite[1], Giovanni Martucci[1], Jakub Bialek[1] Ciaran Monahan[1], Harald Berresheim[1], Aditya Vaishya[1], Tomas Grigas[1], S. Gerard Jennings[1], Philip McVeigh[1], Saji Varghese[1], Robert Flanagan[1], Damien Martin[1], Eoin Moran[2], Keith Lambkin[2], Tido Semmler[2], Cinzia Perrino[3], Ray McGrath[2]

[1] School of Physics & Centre for Climate and Air Pollution Studies, Ryan Institute, National University of Ireland Galway, University Road, Galway, Ireland
[2] Met Éireann, Glasnevin Hill, Dublin 9, Ireland
[3] Institute for Atmospheric Pollution, National Research Council, 1-00015 Montelibretti, Rome, Italy

Citation: O'Dowd, C. et al., 2012. The Eyjafjallajökull ash plume – Part I: Physical, chemical and optical characteristics. *Atmospheric Environment*, 48, pp.129–142.
DOI: 10.1016/j.atmosenv.2011.07.004

Atmospheric Environment xxx (2011) 1–14

Contents lists available at ScienceDirect

Atmospheric Environment

journal homepage: www.elsevier.com/locate/atmosenv

The Eyjafjallajökull ash plume – Part I: Physical, chemical and optical characteristics

Colin O'Dowd [a,*], Darius Ceburnis [a], Jurgita Ovadnevaite [a], Giovanni Martucci [a], Jakub Bialek [a], Ciaran Monahan [a], Harald Berresheim [a], Aditya Vaishya [a], Tomas Grigas [a], S. Gerard Jennings [a], Philip McVeigh [a], Saji Varghese [a], Robert Flanagan [a], Damien Martin [a], Eoin Moran [b], Keith Lambkin [b], Tido Semmler [b], Cinzia Perrino [c], Ray McGrath [b]

[a] School of Physics & Centre for Climate and Air Pollution Studies, Ryan Institute, National University of Ireland Galway, University Road, Galway, Ireland
[b] Met Éireann, Glasnevin, Glasnevin Hill, Dublin 9, Ireland
[c] Institute for Atmospheric Pollution, National Research Council, I-00015 Montelibretti, Rome, Italy

ARTICLE INFO

Article history:
Received 5 February 2011
Received in revised form
1 July 2011
Accepted 4 July 2011

Keywords:
Volcanic ash plume
Aerosol
Dispersion
Mace Head

ABSTRACT

The Eyjafjallajökull ash plume was detected at the Mace Head Atmospheric Research Station numerous times from April 19th till 18th May 2010 following subsidence into, and dilution in, the boundary layer. The three strongest of these events, lasting 12–18 h, are analysed in detail in terms of physical, chemical and optical properties. The ash size distribution was bimodal with a supermicron mode of 2.5 μm diameter for the one case where it was measured. The submicron mode varied from 185 nm during the high-explosive phase to 395 nm during the low-explosive phase. Non-sea-salt (nss)-sulphate mass was 2.5 times higher during the low-explosive phase. Total particle concentrations ranged from 760 cm^{-3} to 1247 cm^{-3} and were typical of clean air in the region. Between 30% and 39% of submicron chemical mass (i.e. exclusive of water content) was ash primarily composed of silicon dioxide while accounting for the water content, the submicron aerosol was composed of primary ash (15%), nss-sulphate (25%) and water (55%). Hygroscopic growth factors were characteristic of sulphate aerosol but revealed an internally-mixed aerosol pointing to a mix of predominantly primary ash, nss-sulphate and water. For the majority of the ash plumes, all condensation nuclei (CN, diameter > 10 nm) were activated into cloud condensation nuclei (CCN) at a supersaturation of 0.25%. Aerosol absorption increased by about a factor of two in the plume, compared to background levels, while aerosol scattering coefficients increased by an order of magnitude.

1. Introduction

The Eyjafjallajökull volcano erupted explosively on the 14th April 2010, ejecting an ash plume in the atmosphere at levels between 4 km and 9 km a.m.s.l.. While the Eyjafjallajökull eruption was moderate and regarded as a mid-sized eruption (Pyle, 1999; Davies et al., 2010), it had a severe impact on aviation over Europe. The eruption occurred under north–north-westerly air flow, relative to continental Europe and under conditions of minimal precipitation resulting in rapid dispersion of the ash cloud over Central Europe, Ireland and Britain. Based on plume mass estimates from the European Volcanic Ash Advisory Centers, the European aviation authorities decided to close European airspace, impacting air traffic to 23 European countries amounting to a 75% closure of the European aerodrome network. The net effect was that more than 100,000 flights were cancelled, affecting 10 million passenger journeys between the 14th April and 20th April. Further incursions of the ash cloud over Western Europe caused additional airspace closures, sporadically, until the 18th May 2010, leading to the cancelling of about 7000 further flights. Decisions on fly or no-fly centred around an ash mass concentration of 2–4 mg m^{-3}, although no robust in-plume measurements of mass concentrations were achieved in practice. Perhaps the closest plume encounters were achieved by the DLR Falcon aircraft where plume mass concentrations of 1 mg m^{-3} were briefly achieved (Schumann et al., 2011). The unexpected eruption and impact revealed several deficits in Europe's capabilities in terms of accurately detecting and predicting the ash plume mass density, thickness and vertical

* Corresponding author.
E-mail address: colin.odowd@nuigalway.ie (C. O'Dowd).

1352-2310/$ – see front matter © 2011 Elsevier Ltd. All rights reserved.
doi:10.1016/j.atmosenv.2011.07.004

distribution (particularly in terms of layering effects) in near real-time.

This study presents an analysis of the physico-chemical properties of volcanic plume aerosol detected at the Mace Head Supersite on the west coast of Ireland during the period from the 19th April to the 18th May 2010 and builds on recent work characterising the properties of aerosols associated with passive Icelandic volcano emissions (Ovadnevaite et al., 2009). In particular, the relative contributions of primary ash to sulphate, the water fraction, the state of mixing, and the water uptake and cloud condensation nuclei properties are probed in detail. An overview of the eruption storeyline and emission flux is provided in this special issue by Langmann et al. (in this issue).

2. Experimental

Ground based *in-situ* and remote sensing measurements of the plume characteristics were conducted at the Mace Head Atmospheric Research Station. The Mace Head Atmospheric Research Station is located in Connemara, County Galway on the Atlantic Ocean coastline of Ireland at 53° 19′36″N, 9° 54′14″W and offers a clean sector from 190° through west to 300°. Meteorological records show that on average, over 60% of the air masses arrive at the station in the clean sector (Jennings et al., 2003; O'Connor et al., 2008). Air is sampled at 10 m height from a main air inlet positioned at 80–120 m from coastline (depending on tide) (http://www.macehead.org).

A Jenoptik CHM15k ceilometer was used to detect the vertical distribution of the ash plume. The ceilometer measures atmospheric target backscatter profiles over the nominal range 30 m–15 km with first overlap height at around 30 m (full overlap at 1500 m). The measuring principle is LIDAR-based with photon counting recording system and solid-state Nd:YAG laser source emitting at the 1064 nm wavelength. The operating range is 15 km where it can reliably detect lower cloud layers as well as cirrus clouds. The highest vertical resolution is 15 m at which it can detect full vertical profiles of aerosol backscatter and cloud height, boundary layer height and visibility. The ceilometer is calibrated using a multi-wavelength sunphotometer measuring the optical depth of the atmosphere above the ceilometer. Once the calibration is performed the signal is inverted using the Klett algorithm (Klett, 1981) assuming a LIDAR ratio of $S = 42$ sr for $\lambda = 1064$ nm (Ackermann, 1998). The backscatter coefficient is then determined and used to calculate the extinction coefficient through the assumed LIDAR ratio.

Aerosol absorption was measured using a Multi-Angle Absorption Photometer (MAAP). Cloud condensation nuclei (CCN) concentration was determined using a Droplet Measurements Technology CCN counter (Lance et al., 2006) operated at supersatuations of 0.25%, 0.5% and 0.75%.

On-line aerosol analysers sampled from a 10 m height 10 cm diameter laminar flow community duct with a 50% size cut at 3.5 μm at 10 m s^{-1} (Kleefeld et al., 2002). Total particle concentrations at sizes larger than 3 and 10 nm diameter were sampled using a Thermo Systems Inc. (TSI) Condensation Particle Counter (CPC) 3025a and 3010, respectively. Size distributions were sampled using a TSI nano-Scanning Mobility Particle Sizer (SMPS) between 3 and 20 nm, scanning every 30 s, and a standard SMPS operating 10-min size distribution scans between 20 and 500 nm (Wang and Flagan, 1990).

Aerosol scattering coefficient measurements were performed by a TSI 3563 3-wavelength integrating nephelometer (Bodhaine et al., 1991). Supermicron particles were measured using a TSI Aerodynamic Particle Sizer (APS) 3321 which had 51 channel of equal logarithmic width of 0.031 within the size range of 0.54–20.0 μm.

Table 1
Aerosol physical, chemical and optical properties associated with the three strongest plumes detected at Mace Head.

		Case		
		1	2	3
		08:05–12:35 UTC 20/04/2010	17:25 UTC 4/05/2010–02:05 UTC 5/05/2010	17:15–22:25 UTC 17/05/2010
SO_4, μg m^{-3}		2.1 ± 0.2	7.8 ± 0.3	7.2 ± 0.8
NH_4, μg m^{-3}		0.2 ± 0.04	0.18 ± 0.07	0.22 ± 0.06
NO_3, μg m^{-3}		0.04 ± 0.006	0.03 ± 0.005	0.07 ± 0.02
Org, μg m^{-3}		0.2 ± 0.05	0.45 ± 0.09	0.6 ± 0.1
PM2.5 (TEOM), μg m^{-3}		9.1 ± 1.3	10.4 ± 0.9	14.6 ± 1
PM2.5 (SMPS + APS), μg/m^3		–	–	37.7 ± 0.6 16.9 (no water[a])
PM10 (SMPS + APS), μg/m^3		–	–	46.9 ± 0.6 21.1 (no water[a])
Accumulation mode diameter, nm		185 ± 4	380 ± 2	390 ± 4
CN (CPC3010), 1 cm^{-3}		1247 ± 472	762 ± 111	993 ± 295
CN (SMPS), 1 cm^{-3}		732 ± 90	957 ± 213	1070 ± 196
CCN				
SS 0.25%	Nccn, 1 cm^{-3}	424 ± 38	684 ± 62	804 ± 88
	CCN/CNcpc	0.34	0.9	0.81
	CCN/CNsmps	0.58	0.71	0.75
SS 0.5%	Nccn, 1 cm^{-3}	496 ± 45	781 ± 64	896 ± 92
	CCN/CNcpc	0.4	1	0.9
	CCN/CNsmps	0.68	0.82	0.84
SS 0.75%	Nccn, 1 cm^{-3}	622 ± 63	852 ± 80	912 ± 109
	CCN/CNcpc	0.5	1.12	0.92
	CCN/CNsmps	0.85	0.89	0.85
Absorption, Mm^{-1}		0.36 ± 0.1	0.29 ± 0.08	0.38 ± 0.07
Scattering, Mm^{-1}				
450 nm		17.1 ± 0.5	85 ± 6	122 ± 10
550 nm		14.4 ± 0.3	61 ± 5	96 ± 7
700 nm		9.4 ± 0.2	28 ± 3	50 ± 3
Growth factor				
75 nm		1.58 ± 0.05	1.44 ± 0.14	1.58 ± 0.05
165 nm		1.7 ± 0.006	1.64 ± 0.03	1.65 ± 0.03

[a] Excluding particle bound water.

Please cite this article in press as: O'Dowd, C., et al., The Eyjafjallajökull ash plume – Part I: Physical, chemical and optical characteristics, Atmospheric Environment (2011), doi:10.1016/j.atmosenv.2011.07.004

The APS was installed on May 16th, therefore, only data for the latest major plume (17th May) was available.

Hygroscopic properties of aerosol were measured using a Hygroscopic Tandem Differential Mobility Analyzer (H-TDMA), as described by Nilsson et al. (2009) and references therein. The determination of particles growth factor (GF) is done by comparison of sizes of particles in their dry (RH = 40%) and humidified state (RH = 90%). An inversion algorithm is used to retrieve the GF-Probability Density Function (PDF) (Gysel et al., 2009). GFs were measured for 35, 50, 75, 110, 165 nm particle sizes.

The size resolved non-refractory chemical composition of ambient submicron aerosol particles was measured with an Aerodyne High-Resolution Time-of-Flight Aerosol Mass Spectrometer (HR-ToF-AMS). The HR-ToF-AMS focuses aerosol particles in the size range 50–600 nm quantitatively onto a hot surface (~600 °C) using an aerodynamic lens assembly (Jayne et al., 2000). The HR-ToF-AMS was deployed in the standard configuration (DeCarlo et al., 2006), taking both mass spectrum (MS) and particle time-of-flight (pToF) data. HR-ToF-AMS was routinely calibrated according to the methods described by Jimenez et al. (2003) and Allan et al. (2003).

Samples for physical and morphological investigation of volcanic ash were analysed using SEM (Scanning Electron Microscope) with EDX (Energy Dispersive X-ray) chemical analysis method. Samples were taken during two events (19th–20th April and 17th–18th May) and were collected on Whatman cellulose filters. Six 2-h samples were analysed during the April period and five 2-h samples were analysed during the May period. The samples were placed on studs covered with conductive carbon tape and coated with gold for 3 min. All six samples were stored in clean containers to minimize contamination before or during analysis.

Bulk off-line chemical analysis was conducted by the X-ray fluorescence method (XRF) designed to measure elemental composition of aerosol particles irrespective of their chemical make-up. The following elements were analysed: Al, Ca, Cl, Cu, Cr, Fe, K, Mg, Mn, Na, Ni, Pb, Si, S, Ti, V, Zn. The analysis was done for six PM2.5 samples and four PM2.5–10 samples. PM2.5 and PM2.5–10 data from the May 17th are used in this study to reconstruct mass size distribution while other data will be published in a companion paper. In order to calculate ash content and nss-sulphate it was assumed that most of the elements were present in their main oxide forms, sulphur was present in the form of sulphate while sea-salt was calculated as 3.2 × Na.

The 3-dimensional regional climate model, REMOTE (Langmann et al., 2008; Varghese et al., 2011) was used to model volcanic ash dispersion from the Eyjafjallajökull volcano. First, an emission source parameterisation was incorporated to include the time and height dependent emission flux from various levels above the volcano. Then, the aerosol dynamics model M7 (Vignati et al., 2004) was adapted to include the volcanic dust (primary ash) emitted at

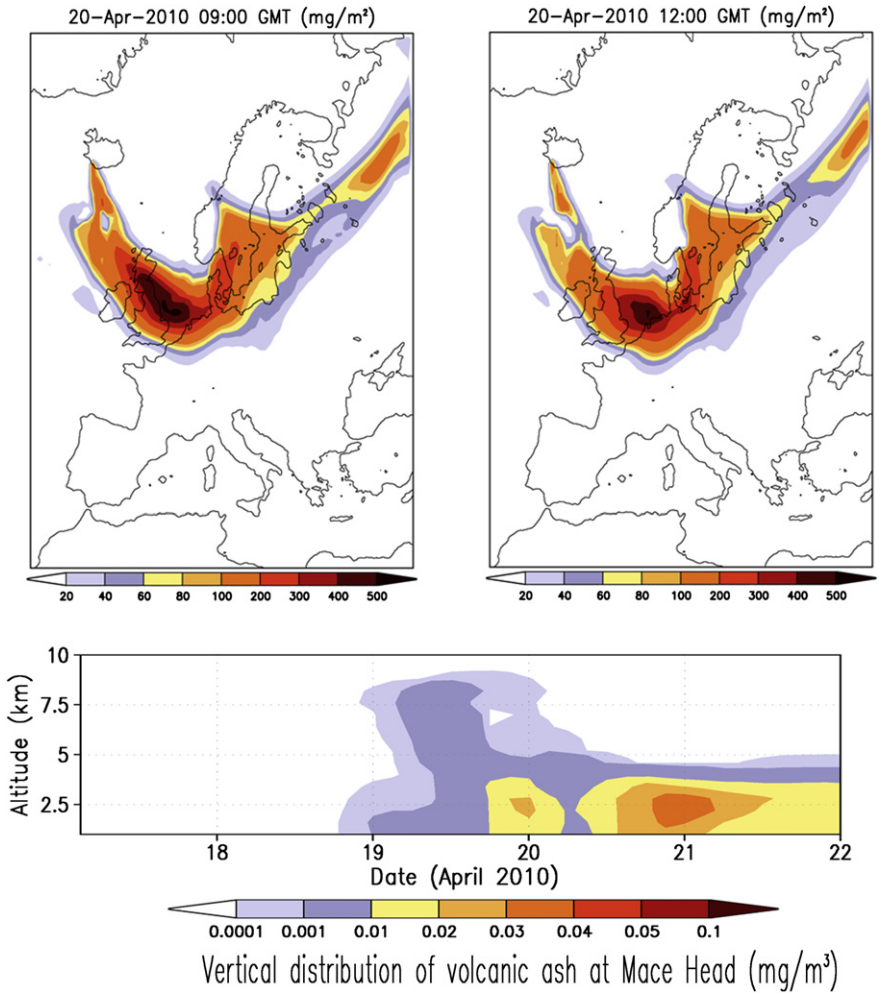

Fig. 1. (Top Left and Right) Spatial distribution of ash plume integrated column mass. (Bottom) Vertical distribution of ash plume volumetric mass concentration. Hindcasting is from the REMOTE model for 20th April 2010.

Please cite this article in press as: O'Dowd, C., et al., The Eyjafjallajökull ash plume – Part I: Physical, chemical and optical characteristics, Atmospheric Environment (2011), doi:10.1016/j.atmosenv.2011.07.004

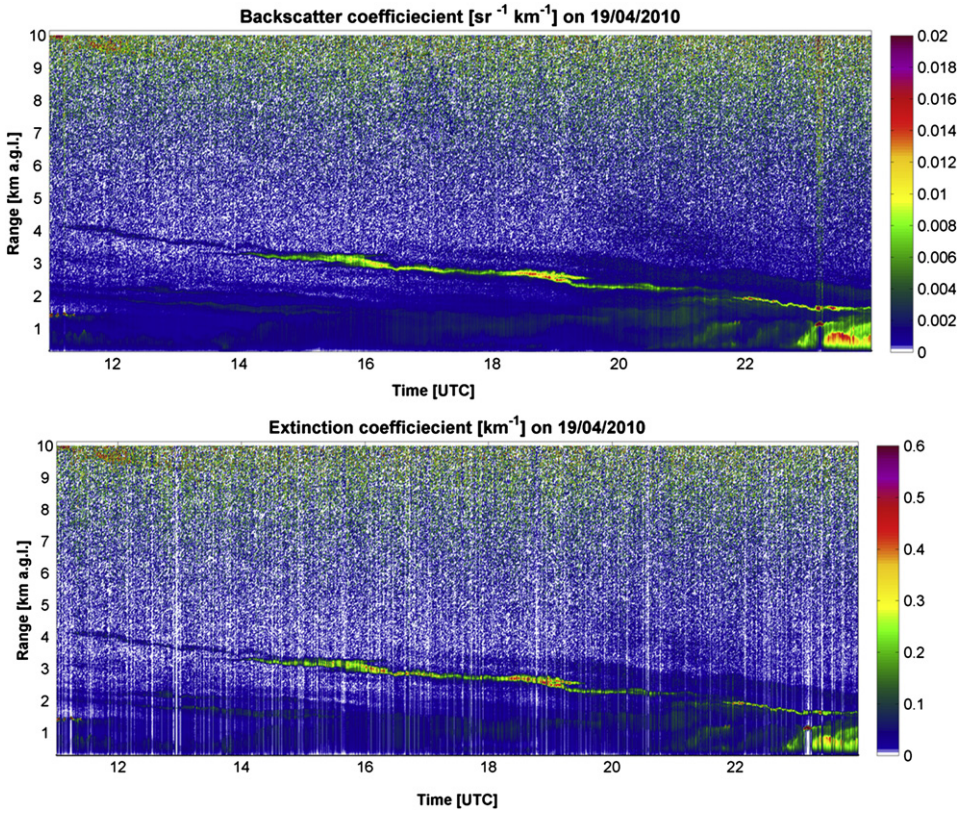

Fig. 2. Temporal evolution of volcanic plume backscatter coefficient (top) and extinction (bottom) over Mace Head on the 19th April. Data derived from the Jenoptik ceilometer.

the source in terms of particle size distribution and density. The emission source parameters are from the EMEP (https://wiki.met.no/emep/emep_volcano_plume). These data are based on tephra estimates derived from preliminary thickness data obtained which was measured on the 17th April at two locations 20 and 50 km east of the volcano and agreed well with theoretical relationships derived for eruption height and volumetric flux for a number of volcanoes. Size distribution measurements of these samples allow size dependent estimates of emission rates. These derived PM10 emissions used for model parameterisation during the relevant study periods ranged in value from 7×10^6 g s^{-1} (19th April) to 2×10^6 g s^{-1} (17th May).

The model was used both as a forecast as well as a hindcast tool (with re-analysis data) for research purposes. Hindcast results were compared, and found to be in good agreement, with observations and results from other dispersion models as part of the validation process which are described in detail in Part II of this paper O'Dowd et al. (in this issue). For all the simulations presented in the study here, global re-analysis data of 0.5° resolution obtained from ECMWF (http://www.ecmwf.int) was used as boundary conditions. Ozonesondes were taken at Valentia, 150 km south of Mace Head, and *in-situ* at Mace Head using a Thermo Scientific model 49i UV ozone analyser.

3. Results

The ash plume aerosol properties associated with the three strong and sustained plumes are tabulated in Table 1 and discussed per case study below.

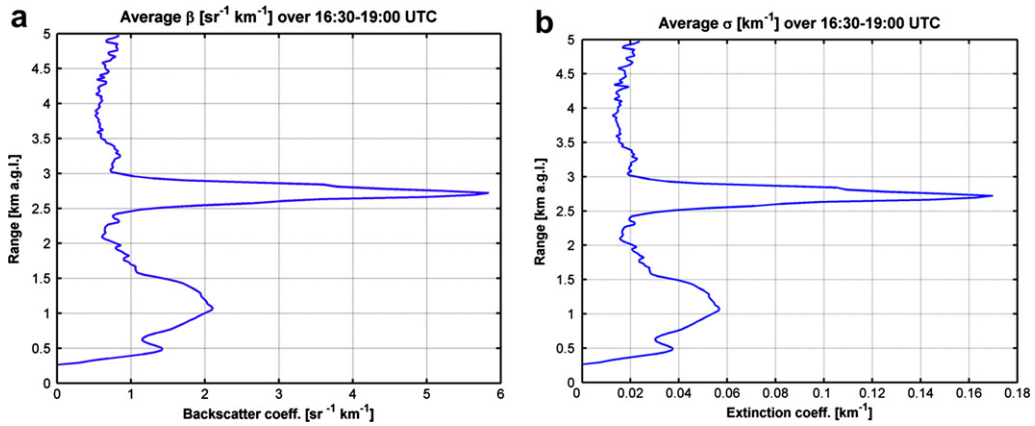

Fig. 3. (a) Vertical profile of backscatter coefficient on 19th April 2010. (b) Vertical profile of extinction coefficient on 19th April 2010.

Please cite this article in press as: O'Dowd, C., et al., The Eyjafjallajökull ash plume – Part I: Physical, chemical and optical characteristics, Atmospheric Environment (2011), doi:10.1016/j.atmosenv.2011.07.004

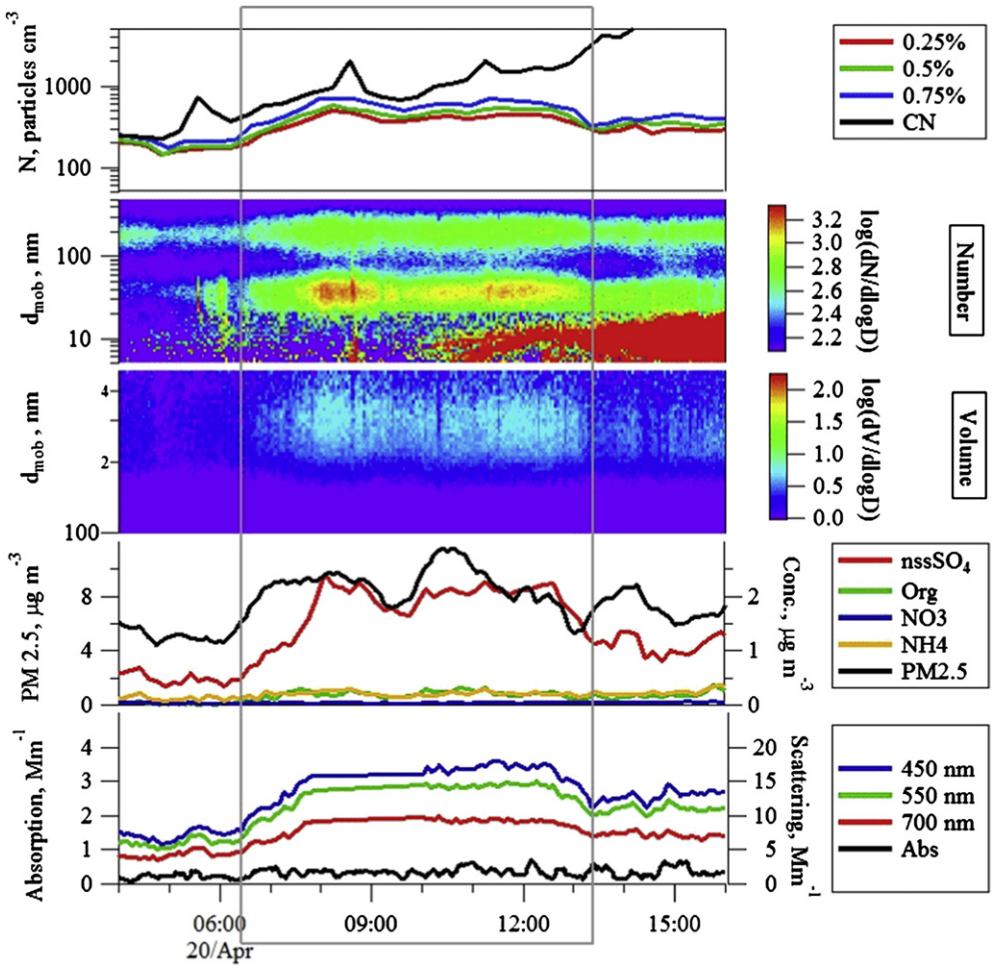

Fig. 4. (Top) Condensation Nuclei (CN) and CCN; (2nd from Top) SMPS aerosol number size distributions; (3rd from Top) SMPS particle volume distributions; (4th from Top) total particulate mass (PM2.5) AMS chemical composition; (Bottom) Aerosol scattering and absorption. The plume period (20th April 2010) is highlighted by the rectangular box.

3.1. Case 1: 19th–20th April 2010

Immediately after the eruption, the plume advected southwest from Iceland and over the north of Britain, into central Europe and then part of it advected west over Ireland in a high pressure system. The dispersion of the plume as simulated by the REMOTE regional climate model is shown in Fig. 1. The hindcast illustrated the maximum density of the plume located over the NE of England on the morning of the 20th April, advecting over the North Sea and Holland by midday of the 20th. The edge of the plume passes over Mace Head during these periods.

The plume was first detected around midday on the 19th April 2010 over Mace Head using the ceilometer (Fig. 2). A thin layer, approximately 200 m thick was detected at an altitude of 4 km and was observed to subside over the subsequent 12 h period after which it entered the boundary layer and was mixed to the surface level. The average vertical profile of backscatter coefficient and extinction from 16:50–17:00 h is shown in Fig. 3. The backscatter coefficient reached a maximum of 0.075 sr km^{-1} while extinction peaked at 1.5 km^{-1} (Fig. 3).

Around midnight of the 19th/20th, as the plume subsided into the boundary layer, aerosol absorption increased from a background level of less than 0.2 Mm^{-1} to a plume average of 0.36 Mm^{-1} while the scattering coefficient, for the blue wavelength, increased from less than 10 Mm^{-1} up to ~17 Mm^{-1} (See Fig. 4). During these periods, PM2.5 increased to ~9.1 μg m^{-3}. The

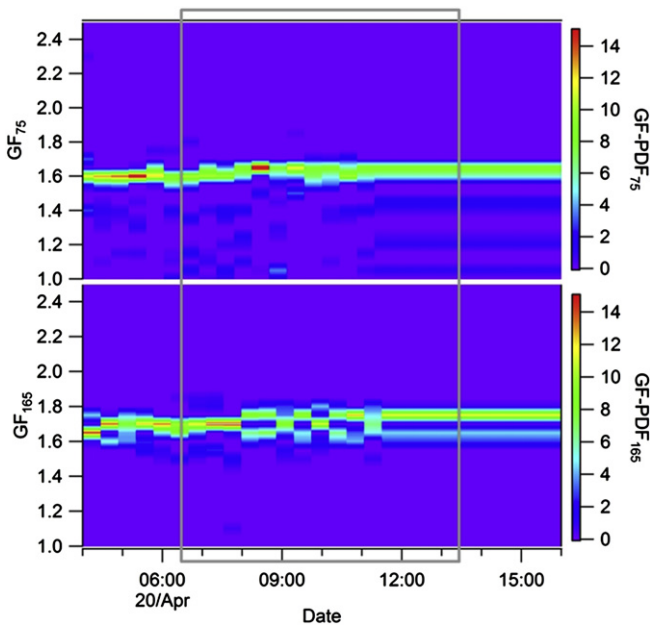

Fig. 5. Hygroscopic growth factors for 75 nm and 165 nm particle sizes.

Please cite this article in press as: O'Dowd, C., et al., The Eyjafjallajökull ash plume – Part I: Physical, chemical and optical characteristics, Atmospheric Environment (2011), doi:10.1016/j.atmosenv.2011.07.004

AMS revealed a relatively large increase in nss-sulphate mass, up to 2.1 μg m^{-3}, with no associated increase in either nitrate or organic aerosol mass. The nss-sulphate mass mode was located at 500–600 nm diameter. Aerosol average concentration for the plume duration was 1247 cm^{-3}. The plume detection revealed a strong accumulation mode with mode diameter at 185 nm, and a strong Aitken mode at 30–40 nm. Before and after the plume was detected, polluted air prevailed and both nucleation and growth events were observed. The CCN (0.75%) concentration was 622 cm^{-3} under plume conditions with a CCN/CN ratio of 0.5. It should be pointed out that an earlier detection of the plume for slightly shorter duration revealed that CCN concentrations at all supersaturations less than 0.75% were equal and the CCN/CN ratio was 1. This indicated that the volcanic aerosol were all very soluble and quite large in size such that no Kelvin effect could be detected. The higher CCN/CN ratio in the case presented appears to be due to the presence of an ultrafine aerosol typically associated with coastal particle production events. This ultrafine mode leads to elevated particle concentrations at sizes of less than 30–50 nm. The aerosol growth factor spanned from 1.58 for 75 nm sizes to 1.7 for 165 nm sizes, pointing to a strong sulphate growth factor signature (Fig. 5) and indicated an internally-mixed aerosol population. There were almost no particles with solubility less than that associated with sulphate aerosol. The high growth factors associated with the ash plume are indicative of a significant sulphate aerosol, even it is internally mixed with crustal ash and activation occurred at a low supersaturation of the order of 0.25%.

3.2. Case 2: 2nd–5th May 2010

The second major plume interaction occurred over the period from 2nd to 5th May 2010. The vertical and horizontal dispersion of the ash plume over Europe is shown in Fig. 6. The hindcast indicates almost direct connected flow between Iceland and Ireland/UK on the 4th–5th May 2010. This flow occurs in very clean polar air. The western edge of the ash plume flows over Mace Head with the most dense part of the plume flowing over Northern Ireland and the Irish Sea.

The case on the 4th of May is selected as it is not only one of the strongest encountered; it is steady for almost 18 h in duration. The temporal and vertical structure of the plume extent over Mace Head, in terms of backscatter coefficient and extinction, is shown in Figs. 7 and 8 for the period preceding subsidence into the boundary layer on the 3rd May. Three layers of elevated backscatter and

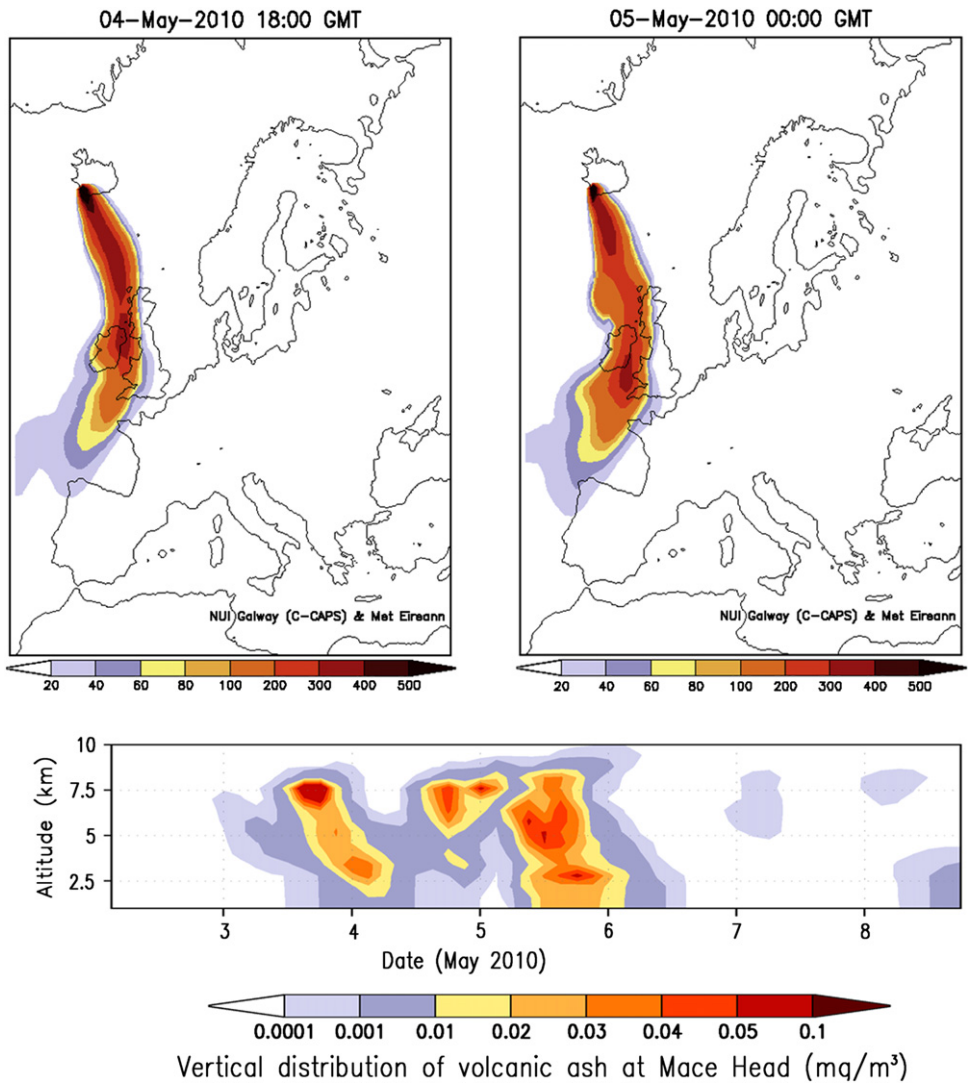

Fig. 6. (Top Left and Right) Spatial distribution of ash plume integrated column mass. (Bottom) Vertical distribution of ash plume volumetric mass concentration. 4th–5th May 2010.

Please cite this article in press as: O'Dowd, C., et al., The Eyjafjallajökull ash plume – Part I: Physical, chemical and optical characteristics, Atmospheric Environment (2011), doi:10.1016/j.atmosenv.2011.07.004

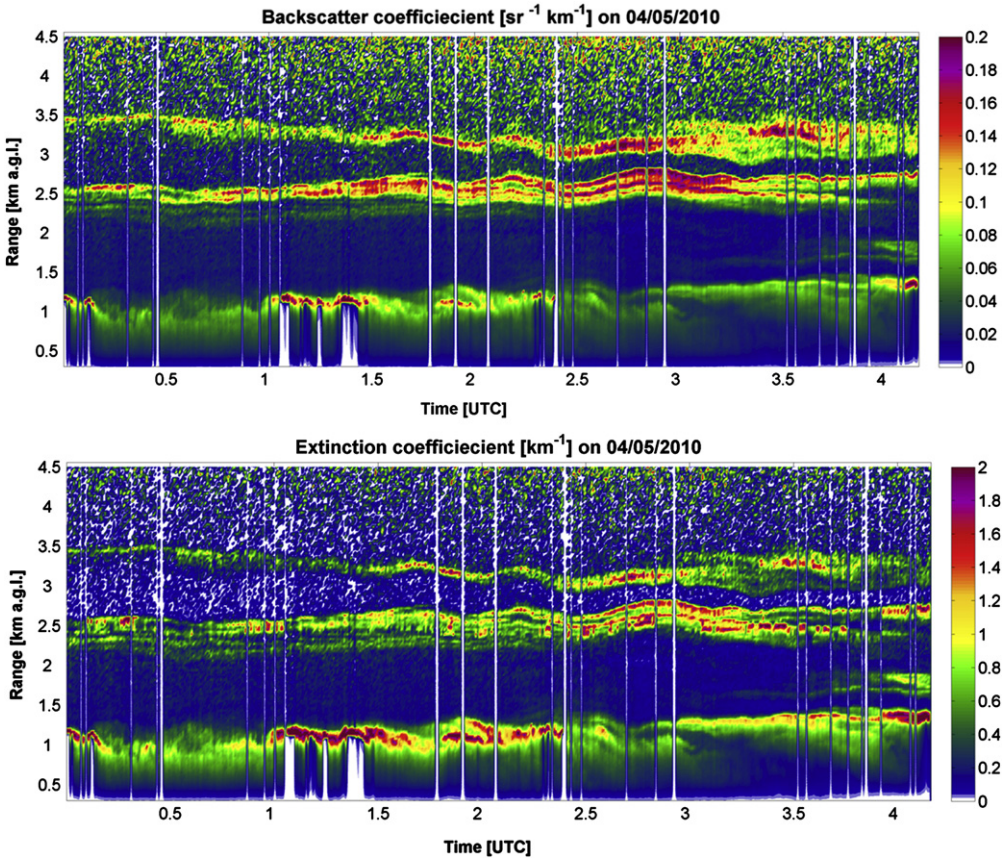

Fig. 7. Temporal evolution of volcanic plume backscatter coefficient and extinction coefficient over Mace Head on the 3rd May.

extinction coefficients are evident in the figures. At approximately 1 km, boundary layer aerosol is evident whilst two distinct and stratified volcanic plume layers are observed at 2.5 and 3.5 km altitude. Again, these layers extend 200–300 m in the vertical.

The backscatter coefficient extends to 0.14 sr km^{-1} while the extinction peaks slightly above 1 km^{-1}. The backscatter coefficient in the plume layers is significantly higher than that in the boundary layer while the boundary layer extinction is nearly equivalent to the ash plume extinction in this case. Total particle concentration was less than 780 cm^{-3} and the CCN/CN ratio was approximately 1 for all supersaturations measured (Fig. 9). The almost 100% activation ratio at the lowest supersaturation of 0.25% points to a large nuclei size composed of very soluble material at the surface despite the possibility of an insoluble volcanic ash core.

The optical properties do not exhibit notable increases in absorption; however, the scattering coefficient increases from background levels of less than 10 Mm^{-1} to 28 Mm^{-1} for the red wavelength and to 85 Mm^{-1} for the blue wavelength. Concomitant with the increase in scattering, total PM2.5 increased to >10.4 μg m^{-3}, although it should be noted that this mass concentration is not unusual in either clean or polluted air at Mace Head. What is unusual, and provides the ash plume signature is the 7.8 μg m^{-3} nss-sulphate aerosol without any elevation in organic or nitrate aerosol mass. Again, the accumulation mode diameter

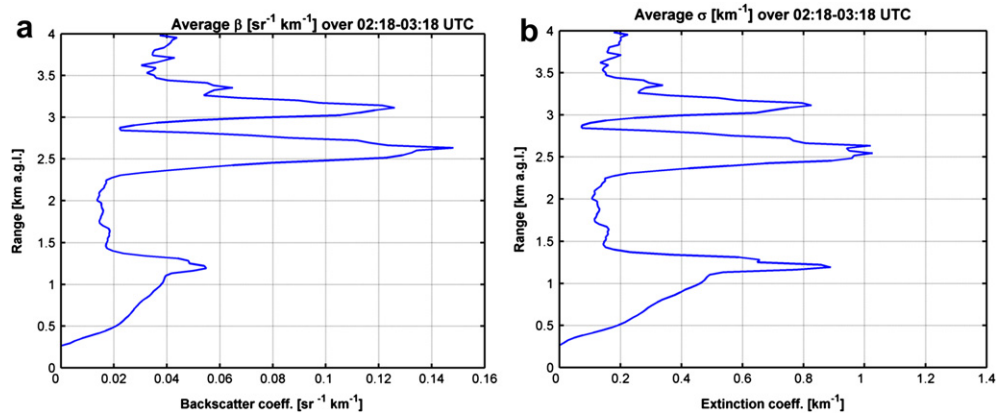

Fig. 8. (a) Vertical profile of backscatter coefficient on 3rd May 2010. (b) Vertical profile of extinction coefficient on 3rd May 2010.

Please cite this article in press as: O'Dowd, C., et al., The Eyjafjallajökull ash plume – Part I: Physical, chemical and optical characteristics, Atmospheric Environment (2011), doi:10.1016/j.atmosenv.2011.07.004

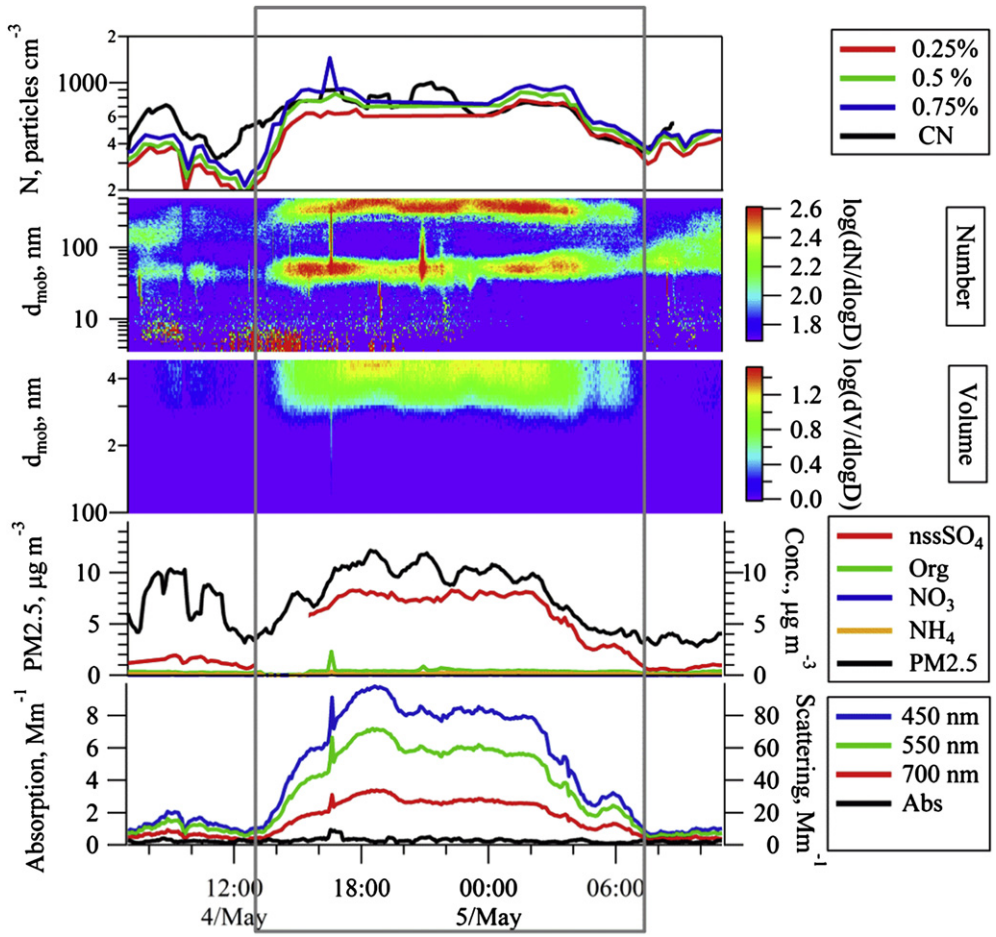

Fig. 9. (Top) Condensation Nuclei (CN) and CCN; (2nd from Top) SMPS aerosol number size distributions; (3rd from Top) SMPS particle volume distributions; (4th from Top) total particulate mass (PM2.5) AMS chemical composition; (Bottom) Aerosol scattering and absorption. The plume period (4th–5th May 2010) is highlighted by the rectangular box.

was ~380 nm. The hygroscopic growth factor probability distribution function, at all sizes, revealed almost 100% GFs of between 1.44 and 1.64, indicating a quite pure nss-sulphate composition GF, although this does not rule out sulphate-coated insoluble cores.

3.3. Case 3: May 17th–18th

The third strong event observed at Mace Head occurred on the 17th and 18th May 2010. Again, the vertical and horizontal dispersion over Europe is illustrated in Fig. 10, while Fig. 11 displays the plume descending from 4 km towards the boundary layer. The plume dispersion on the 16th and 17th of May was more concentrated over the North Sea, nevertheless, significant concentrations were still forecast over the west coast of Ireland. Also evident in Fig. 11 is boundary layer non-plume aerosol at levels below 1.5 km where stratification is also evident.

Later in the day, stratocumulus cloud forms at between 2.2 and 2.5 km altitude as is evidenced by the vertical profiles of backscatter and extinction coefficients in Fig. 12. Above the cloud, the plume backscatter coefficient approaches 2.5 km^{-1} while the extinction coefficient exceeds 0.4 km^{-1}.

During the plume on the 17th May, the total aerosol concentrations (Fig. 13) decreased from more than 10^4 cm^{-3}, associated with a nucleation and growth event, to about 890 cm^{-3} initially and then further to about 300 cm^{-3}. Again, for most of the duration of the plume, the CCN/CN ratio approaches 1 for all supersaturations up to 0.75% suggesting large and very soluble nuclei. The latter part of the plume had a lower CCN/CN ratio leading to a plume average of 0.81. Nss-sulphate mass for this plume averaged at 7.2 μg m^{-3} while PM2.5 mass was 14.6 μg m^{-3}. Absorption reached a plume average of 0.38 Mm^{-1}, while the red wavelength scattering was 50 Mm^{-1} and the blue wavelength scattering was 122 Mm^{-1}.

Again, a very large accumulation mode, of the order of 390 nm diameter, was present compared to a typical background mode of 120–150 nm diameter (Yoon et al., 2007). For this case, the APS was deployed to measure supermicron size spectra. During the plume the combined SMPS and APS spectrometers reveal two strong mobility mass modes at 560 nm 2.6 μm. The GFs were between 1.58 and 1.65 for all sizes measured. However, examination of the derived mass size spectra exhibits striking differences between the combined APS and SMPS mass and that derived from the TEOM. This will be discussed later.

3.4. Off-line chemical analysis

The off-line PM2.5 and PM10 chemical analysis was speciated according to three main categories, namely, nss-sulphate, sea-salt and ash. The analysis is only presented for the event (24-h average) on the 17th May and results are tabulated in Table 2 where mass concentrations of the categories, exclusive of nitrate, ammonium, organic matter and compounds bound water (as in gypsum, sulphuric acid, etc.) are presented. For this event, the PM10 mass was 11.45 μm m^{-3} of which 33% was sulphate, 39% ash, and 28% sea-salt.

Please cite this article in press as: O'Dowd, C., et al., The Eyjafjallajökull ash plume – Part I: Physical, chemical and optical characteristics, Atmospheric Environment (2011), doi:10.1016/j.atmosenv.2011.07.004

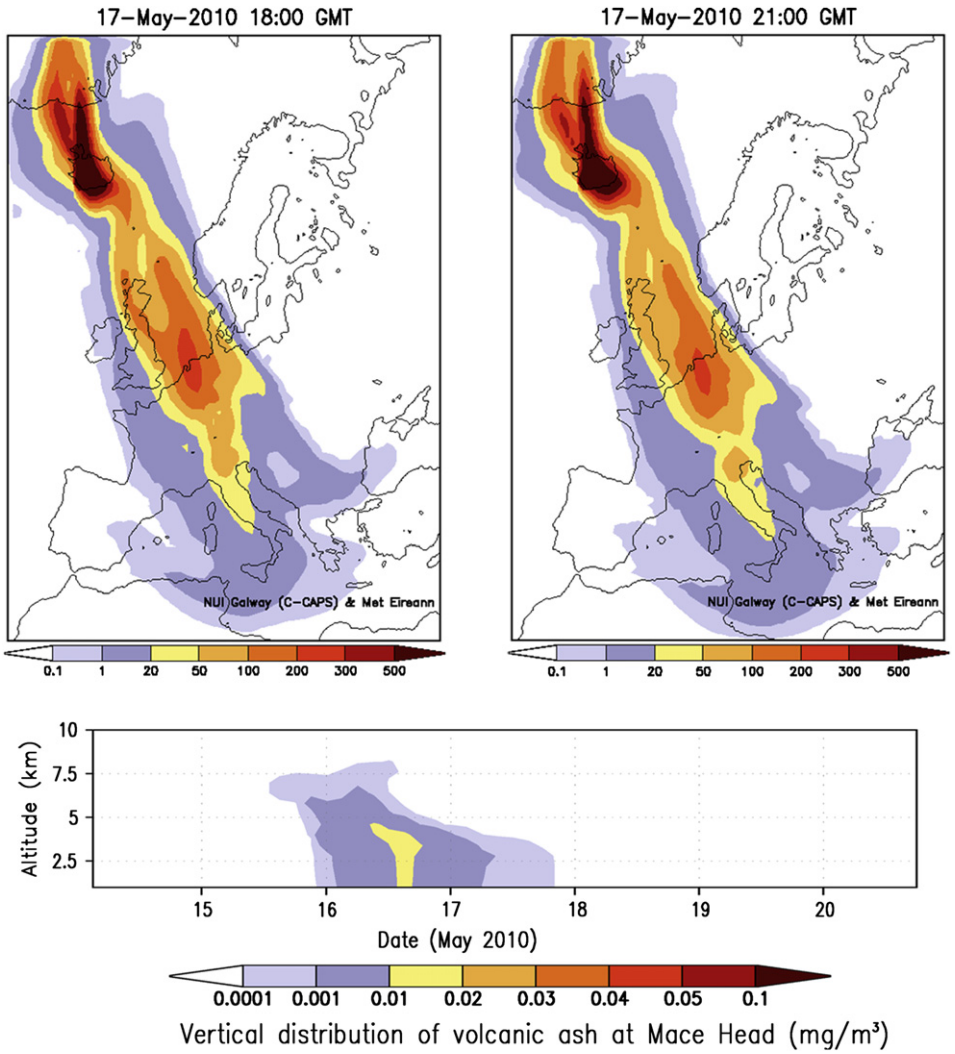

Fig. 10. (Top Left and Right) Spatial distribution of ash plume integrated column mass. (Bottom) Vertical distribution of ash plume volumetric mass concentration. 17th–18th May 2010.

For PM2.5, total mass was 5.03 μm m^{-3} of which 64% was sulphate, 30% ash, and 7% sea-salt.

3.5. Scanning electron microscopy analysis

SEM samples were taken during two events: April 19th–20th (the first volcanic plume reaching Mace Head after explosive eruption on April 14th) and May 17th–18th (the highest nss-sulphate loading and longest in duration event). Volcanic ash SEM analysis of the first volcanic ash plume detected on April 19th revealed a diverse morphology and composition of ash particles, but mainly consisting of silica oxide (Fig. 14a), which also was the dominant oxide in Eyjafjallajökull lava. A large number of particles contained significant amounts of sulphur, indicating secondary processes of sulphate/sulphuric acid formation from sulphur dioxide oxidation during transport in the volcanic plume, also mixed with sea-salt (Fig. 14b) picked up during transport over oceanic regions. Volcanic glass shards (Fig. 14d) were common with the presence of Al, which oxide was the second most abundant in Eyjafjallajökull lava. Melting and re-crystallization of particles (Fig. 14c) was also evident in particles. Many of the particles were incrusted with various metals like Fe, Cr and Ti.

SEM analysis of particles collected during the period of May 17th–18th revealed less diverse composition and the particles in general and were smaller in size than during April 19th–20th period. However, more diverse glass shard particles were detected with entire glassy particles present in samples (Fig. 15b). There was a clear evidence of gypsum forming in the particles rich in calcium oxide when increasing amount of sulphuric acid became available which is evident in Fig. 16 exhibiting twinned crystal shape particle typical of growing gypsum crystal and confirmed by exclusive chemical composition of Ca, S and O.

These differences could indicate that the explosive activity of the volcano was decreasing and less of the bigger particles were ejected to significant height to be later efficiently transported over the long distances. However, melted/re-crystallized/fused particles were present (Fig. 15c and d) which indicated similar particle evolution in the rising volcanic plume as during the beginning of the eruption in April.

3.6. Ozone depletion in the ash plume

On several days when the volcanic plume mixed into the boundary layer down to ground level at Mace Head the rapid

Please cite this article in press as: O'Dowd, C., et al., The Eyjafjallajökull ash plume – Part I: Physical, chemical and optical characteristics, Atmospheric Environment (2011), doi:10.1016/j.atmosenv.2011.07.004

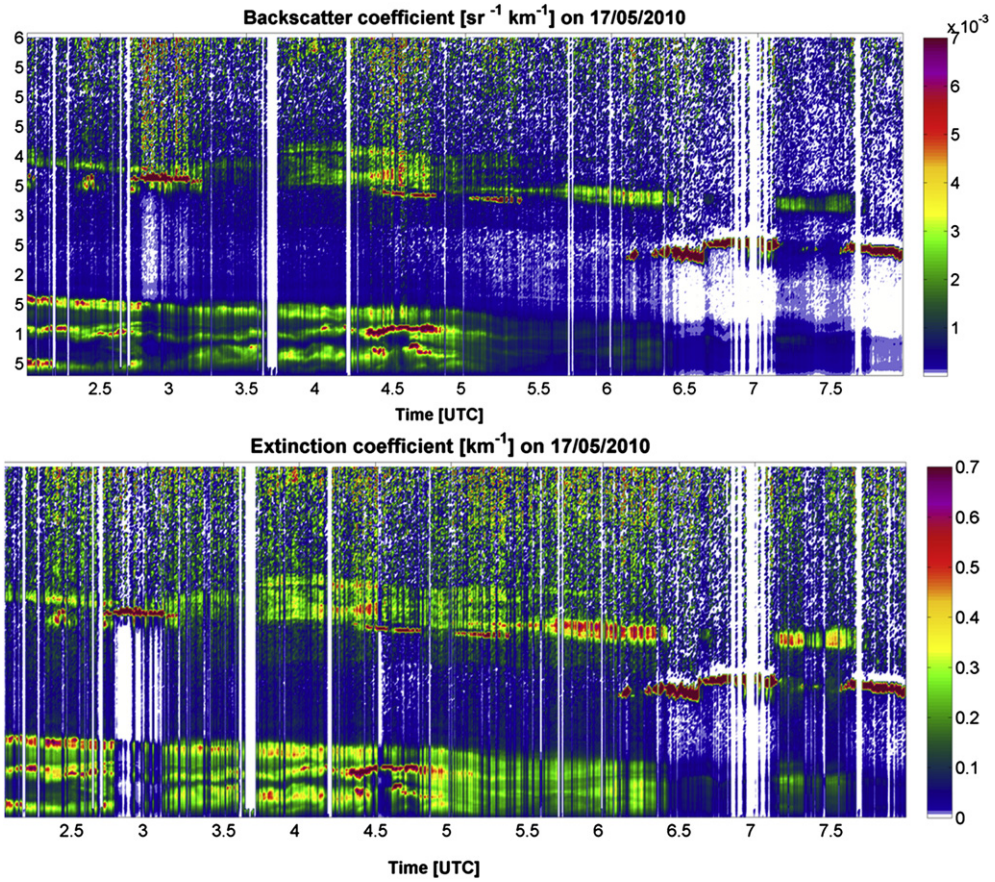

Fig. 11. Temporal evolution of volcanic plume backscatter coefficient and extinction coefficient over Mace Head on the 17th–18th May 2010.

increase in aerosol sulphate concentrations detected by the AMS was accompanied by a conspicuous drop in ground level ozone mixing ratios. A clear example is shown in Fig. 16 for 17th May 2010, when O_3 levels decreased by about 15 ppbv during plume arrival. Ozonesonde profiles launched at 12 GMT from the Valentia Station typically showed O_3 mixing ratios of 40–60 ppbv in the free troposphere (FT) in the absence of the plume over that region (e.g., 19th May). These observations suggested significant ozone depletion within the volcanic plume. Assuming SO_2 levels of 40–100 ppbv at plume altitudes, as observed during flight measurements north of Ireland by Schumann et al. (2011) and Heue et al. (2010), model calculations show that about 80% of the aerosol nss-sulphate concentrations can be explained by in-cloud aqueous phase oxidation dominated by ozone (Flanagan et al., 2011). Sulphate aerosol concentrations in the FT may have been on the order of 50 μg m^{-3} over Ireland in relative agreement with the airborne observations. In addition to in-cloud SO_2 oxidation, further depletion of ozone in the plume could have been caused by rapid bromine chemistry. Heue et al. (2010) measured BrO mixing ratios of 4–6 pptv in the plume on 16 May consistent with significant BrO total column densities retrieved simultaneously from GOME-2 satellite. Previous measurements (Bobrowski et al., 2007,

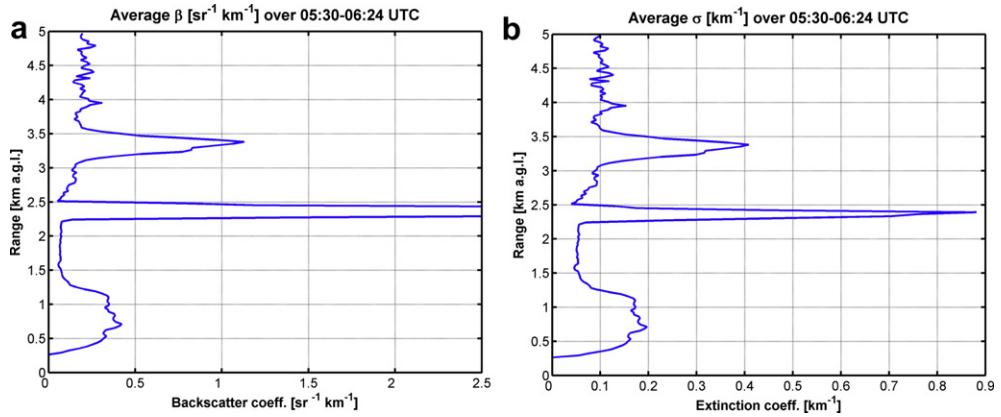

Fig. 12. (a) Vertical profile of backscatter coefficient on 17th May 2010. (b) Vertical profile of extinction coefficient on 17th May 2010.

Please cite this article in press as: O'Dowd, C., et al., The Eyjafjallajökull ash plume – Part I: Physical, chemical and optical characteristics, Atmospheric Environment (2011), doi:10.1016/j.atmosenv.2011.07.004

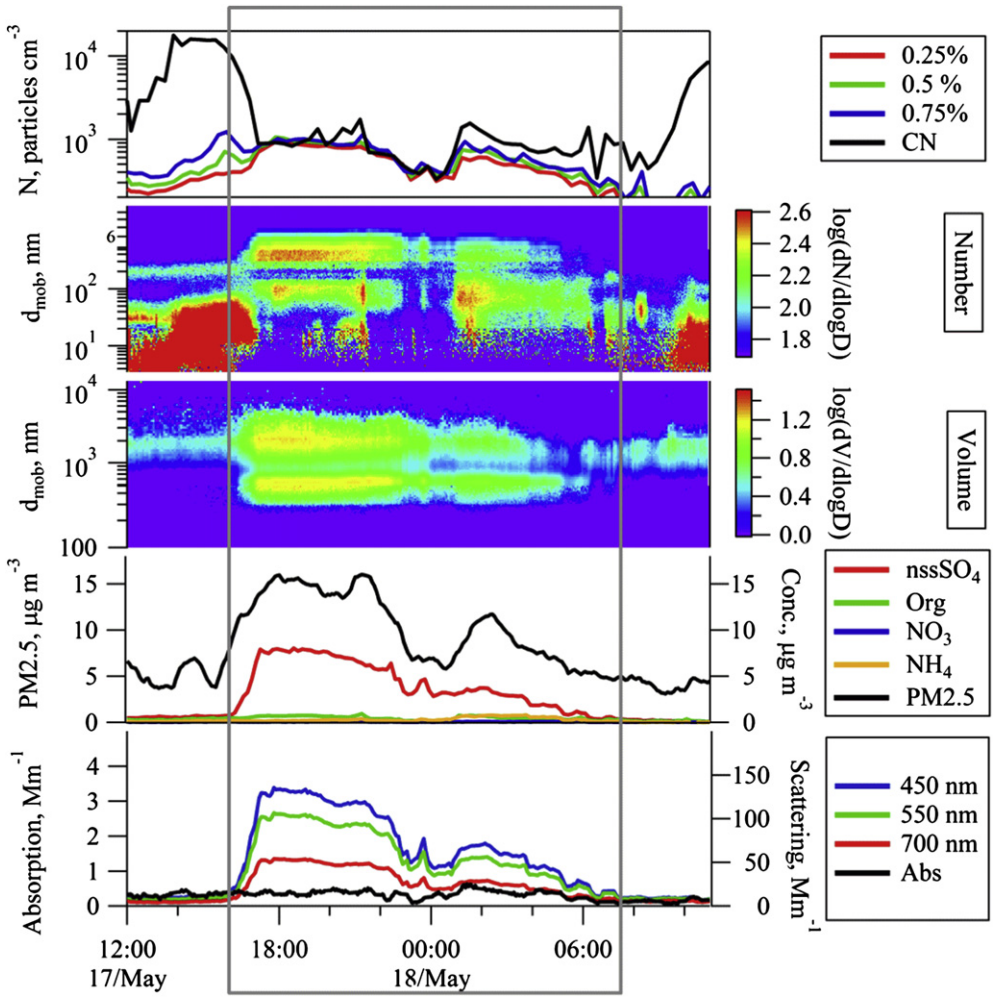

Fig. 13. (Top) Condensation Nuclei (CN) and CCN; (2nd from Top) SMPS aerosol number size distributions; (3rd from Top) SMPS particle volume distributions; (4th from Top) total particulate mass (PM2.5) AMS chemical composition; (Bottom) Aerosol scattering and absorption. The plume period (17th–18th May 2010) is highlighted by the rectangular box.

2003) and model simulations (von Glasow, 2010) have shown that bromine radical reactions in volcanic plumes can deplete ozone down to as much as 10% of its ambient background levels.

4. Discussion

The first plume period reported here represented the high-explosive part of the eruption while the latter two events represent the less-explosive period of the eruption. The high-explosive period was characterised by low SO_2 while the less-explosive period was characterised by high SO_2 emissions as determined by satellite (Evgenia Ilyinskaya, personal communication). During the high-explosive period, the ash has a smaller modal size (185 nm) concomitant with only moderate increases in nss-sulphate mass while for the less-explosive periods, the mode diameter increased to 390 nm and nss-sulphate mass amounted to 7.8 µg m^{-3}.

From the third case presented, and for when the most complete set of instruments were deployed, there were two methods to measure total particulate mass: the first, a TEOM, provided a mass measurements at PM2.5, while, second, the combination of the SMPS and APS single particle size spectrometers were used to derive a mass size distribution based on certain assumptions, including that of density. The TEOM operates on the basis of an oscillating microbalance, while the SMPS operates on particle mobility principles and the APS operates on aerodynamic time-of-flight measurements. To produce a mass distribution from the combination of the SMPS and APS, the APS diameter must be converted into a mobility diameter and a density is applied to the volume distribution to produce a mass distribution. In addition, nss-sulphate mass at PM1 was derived from the AMS and for PM2.5 and PM10 size-cuts, nss-sulphate, ash and sea-salt mass where retrieved through off-line chemical analysis.

The plume on 17th May warrants special attention as the full suite of aerosol measurements at Mace Head were deployed and revealed some intriguing differences between different measurement techniques. During this plume, the PM2.5 mass from the TEOM amounted to 14.6 µg m^{-3}, while mass from the size spectrometers, for PM2.5 mass amounted to 37.7 µg m^{-3}, and for PM10 amounted to 46.9 µg m^{-3}. For the off-line chemical analysis, only

Table 2
Percentage contributions of major compound classes to particulate mass concentrations (24 h averages) during May 17th event derived from XRF analysis.

		nss SO_4, %	Ash, %	Sea-salt, %
PM10[a]	11.45 µg m^{-3}	33	39	28
PM2.5[a]	5.03 µg m^{-3}	64	30	7
PM2.5–10[a]	6.42 µg m^{-3}	10	46	44

[a] PM concentrations exclude nitrate, ammonium, organic matter and compound bound water (as in gypsum, sulphuric acid, etc.).

Please cite this article in press as: O'Dowd, C., et al., The Eyjafjallajökull ash plume – Part I: Physical, chemical and optical characteristics, Atmospheric Environment (2011), doi:10.1016/j.atmosenv.2011.07.004

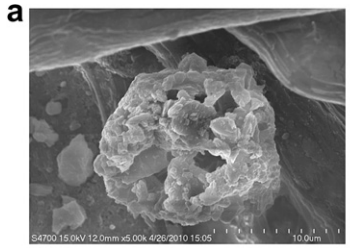

Element	Weight%	Atomic%
C	38.91	54.62
O	24.42	25.74
Si	14.86	8.92
Al	4.15	2.59
Na	2.26	1.66
S	2.96	1.55
Ca	3.60	1.51
Cl	3.13	1.49
Fe	4.28	1.29
K	1.43	0.62

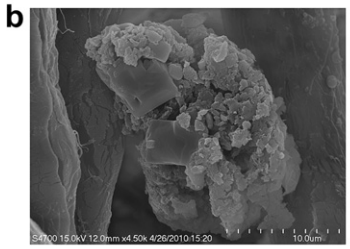

Element	Weight%	Atomic%
C	46.88	59.20
O	31.58	29.94
Si	11.07	5.98
Cl	3.01	1.29
Al	2.06	1.16
Na	1.27	0.84
Mg	0.78	0.48
Fe	1.57	0.43
Ca	1.08	0.41
K	0.71	0.28

Element	Weight%	Atomic%
O	56.95	70.13
Na	8.52	7.30
Cl	11.25	6.25
Mg	6.59	5.34
Al	6.49	4.74
Si	5.66	3.97
K	2.71	1.36
Ca	1.83	0.90

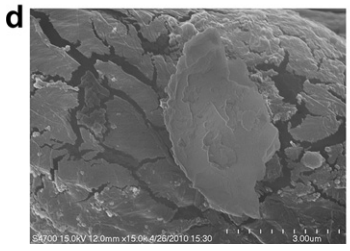

Element	Weight%	Atomic%
C	37.13	47.34
O	44.13	42.24
Si	11.94	6.51
Al	3.41	1.93
Na	2.36	1.57
K	1.03	0.40

Fig. 14. SEM images of volcanic ash particles collected during the period of April 19–20. Carbon in elemental composition stems from cellulose fibres.

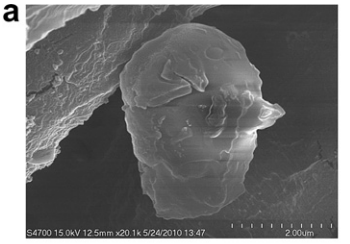

Element	Weight%	Atomic%
O K	21.60	34.50
Na K	2.51	2.79
Al K	9.92	9.39
Si K	47.58	43.28
K K	5.15	3.37
Ca K	3.42	2.18
Fe K	9.82	4.49

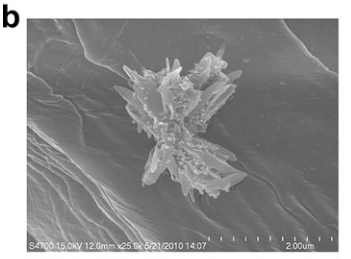

Element	Weight%	Atomic%
C K	54.40	63.88
O K	36.09	31.82
Na K	1.69	1.04
Mg K	0.43	0.25
Al K	0.26	0.14
S K	3.70	1.63
Cl K	0.91	0.36
Ca K	2.51	0.88

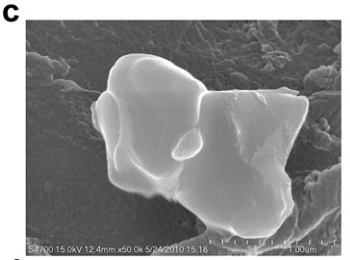

Element	Weight%	Atomic%
O K	60.49	78.76
Na K	2.08	1.89
Al K	5.71	4.41
Si K	8.45	6.27
Fe K	23.26	8.68

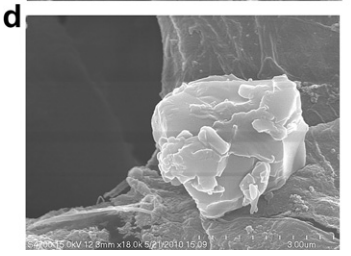

Element	Weight%	Atomic%
C K	15.21	22.82
O K	49.08	55.27
Na K	3.35	2.62
Al K	5.23	3.49
Si K	20.94	13.43
K K	1.40	0.65
Ca K	1.36	0.61
Fe K	3.43	1.11

Fig. 15. SEM images of the particles collected during the period of May 17–18. Carbon in elemental composition stems from cellulose fibres.

ash, sulphate and sea-salt were reported and the total amounted to 5.03 and 11.45 μg m^{-3}, respectively, for PM2.5 and PM10. The latter was averaged over a 24 h period and therefore contains significant time outside the plume, hence the lower concentrations. If one focuses on PM2.5 mass, we have a discrepancy whereby the size spectrometers report mass concentrations more that twice that of the TEOM and the nss-sulphate mass comprises ~50% of the TEOM mass and ~25% of the spectrometer mass. The discrepancy cannot be accounted for by the ash content as the off-line chemical analysis indicated a sulphate to ash ratio of 2:1. Given that the other major chemical constituents amount to perhaps, at most, 10% of the PM2.5 mass, the most rational remaining conclusion is that the missing mass relates to the water content associated with the sulphuric acid aerosol and that this water content had not evaporated in the SMPS and APS, but had evaporated in the TEOM given its operating temperature of 50 °C. Closure between the instruments is achieved if ~55% of the PM2.5 mass is accounted for by water, and the remaining mass is nominally ~30% sulphate and ~15% ash. This results in an average density, considering primarily of nss-sulphate, ash and water, of $\rho = 1.43$ g cm^{-3}. Fig. 17 illustrates the resulting SMPS/APS size distribution compared to the AMS non-refractory spectrum.

Particle bound water was also estimated using E-AIM (Extended Aerosol Inorganics Model) model (http://www.aim.env.uea.ac.uk/

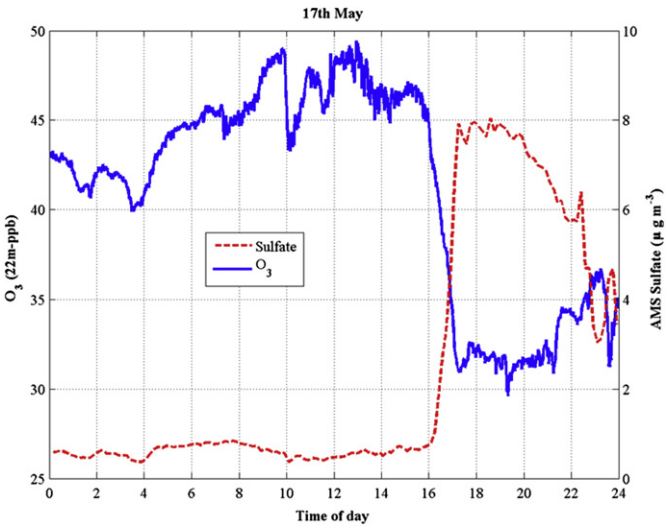

Fig. 16. Ozone and nss-sulphate concentrations as the 17th May 2010 ash plume entered the boundary layer at Mace Head.

Please cite this article in press as: O'Dowd, C., et al., The Eyjafjallajökull ash plume – Part I: Physical, chemical and optical characteristics, Atmospheric Environment (2011), doi:10.1016/j.atmosenv.2011.07.004

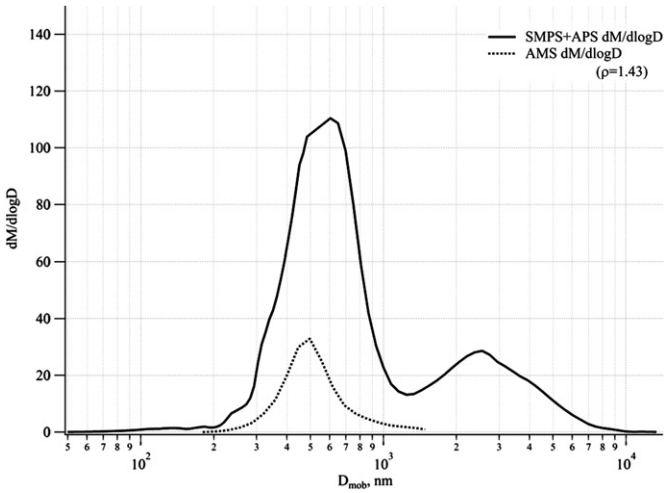

Fig. 17. Volcanic aerosol mass closure. AMS mass size distribution is of total non-refractory mass presented in mobility scale. Mass size distribution of combined SMPS and APS distributions presented in mobility scale. APS aerodynamic and AMS vacuum aerodynamic sizes converted to mobility diameter assuming particle density of 1.43 g cm^{-3}. Mass discrepancy between submicron spectra is due to particle water and refractory ash components.

aim/aim.php) developed by the University of East Anglia (Carslaw et al., 1995; Massucci et al., 1999; Clegg and Brimblecombe, 2005; Clegg et al., 1998). Using chemical species concentrations presented in Table 2 and the range of relative humidities (50–80%) and temperatures (10–15 °C) estimated particle bound water content was in the range of 9.2–25.7 μg m^{-3}. Ambient relative humidity was close to 100% and unspecified drying has occurred in the community sampling duct or the instruments (SMPS and APS). However, equilibrium temperature and RH conditions possibly have not been met during the sampling time scale (~10 s) resulting in water content on a higher end of the estimation which is consistent with the indirect estimate of 20.6 μg m^{-3} of water. The resulting density of particles adding known amount of ash from Table 2 was in the range of 1.32–1.45 g cm^{-3}, consistent with an indirect estimate of 1.43 g cm^{-3}.

Despite being an internal mix of an insoluble ash fraction, the hydroscopic GF is identical to sulphate aerosol and given the large modal sizes, these particles are excellent CCN with typically 100% activation at supeprsaturations as low as 0.25%. The high activation efficiency of the volcanic aerosol was also reflected in ground based remotely-sensed cloud microphysics for one event where it is thought that the ash layer induced the formation of a layered cloud above the boundary layer (Martucci et al., in this issue). In that study, the mean droplet concentration was ~300 cm^{-3}; however, peak concentration of ~1000 cm^{-3} were observed (i.e. similar to maximum CCN concentrations). Gassó (2008) also found major microphysical impacts on low level marine clouds from volcanic emissions on Saunders Island, South Atlantic. The Mount Michael volcano was undergoing a steady and simmering eruption and large reductions in the cloud effective radius was observed from satellite. Yuan et al. (2011) also found similar impacts on marine trade wind cumulus downwind of a gently degassing Hawaiian volcano Kilauea where increases in precipitation associated with reductions of effective radius were observed in clouds forming in-plume enriched air.

Observations of the ash plume were conducted from aircraft (Schumann et al., 2011) and also from ground based stations (e.g., Zugspitze/Hohenpeissenberg, Flentje et al., 2010); however, direct comparison of aerosol properties is not so straight forward as few overlapping parameters. The easiest parameter to compare with is total number concentration. At Mace Head, we observed concentrations of the order of 1000 cm^{-3}, whereas, airborne measurements by Schumann et al. report concentrations in excess of 10,000 cm^{-3} and Flentje et al. only report total particle concentrations as "enhanced or normal". Flentje et al. reported PM10 mass concentrations of the order of 40–50 μg m^{-3}, similar to Mace Head, while airborne measurements by Schumann et al. report mass concentrations as high as 400 μg m^{-3}. Turbulent mixing of the 200 m thick ash plume into a boundary layer approximately 1000 m suggests that the boundary layer ash mass concentrations were likely to be diluted by a maximum factor of 5, indicating that the maximum ash cloud mass concentrations could have approached 250–300 μg m^{-3}.

5. Conclusions

The Eyjafjallajökull aerosol plume was sampled and characterised in terms of physico-chemical properties as it descended into the boundary layer. During the initial intensive explosive phase of the eruption, with low SO_2 emissions, the submicron modal diameter was of the order of 185 nm, while during the less intensive explosive phase, the modal diameter was of the order of 395 nm and the supermicron mode was of the order of 2.5 microns. The supermicron ash chemical composition was primarily silicon oxides and the submicron aerosol was composed of an internal mix of primary ash (15%), nss-sulphate (25%) and water (55%). The physical size and chemical composition result in the ash plume aerosol being very efficient CCN as evidenced by a 100% ratio efficiency for CCN/CN at supersaturations as low as 0.25%. PM10 mass concentrations compare well with other measurements from European ground based stations and are about an order of magnitude lower than that of airborne flight measurements of the plume.

Acknowledgements

The authors would like to acknowledge the following funding agencies/programmes: HEA-PRTLI4, SFI, EPA-Ireland, FP6-EUCAARI, FP6-GEOMON, FP6-EUSAAR; and the CNR-Rome for chemical analysis. Further, the Irish Centre for High End Computing is acknowledged for supercomputing resource support.

References

Ackermann, J., 1998. The extinction-to-backscatter ratio of tropospheric aerosols: a numerical study. J. Atmos. Ocean. Tech. 15, 1043–1050.

Allan, J.D., Alfarra, M.R., Bower, K.N., Williams, P.I., Gallagher, M.W., Jimenez, J.L., McDonald, A.G., Nemitz, E., Canagaratna, M.R., Jayne, J.T., Coe, H., Worsnop, D.R., 2003. Quantitative sampling using an aerodyne aerosol mass spectrometer: 2. Measurements of fine particulate chemical composition in two UK cities. J. Geophys. Res. 108 (D9).

Bobrowski, N., Hönninger, G., Galle, B., Platt, U., 2003. Detection of bromine monoxide in a volcanic plume. Nature 423, 273–276.

Bobrowski, N., von Glasow, R., Aiuppa, A., Inguaggiato, S., Louban, I., Ibrahim, O.W., Platt, U., 2007. Reactive halogen chemistry in volcanic plumes. J. Geophys. Res. 112, D06311. doi:10.1029/2006JD007206.

Bodhaine, B.A., Ahlquist, N.C., Schnell, R.C., 1991. 3-Wavelength nephelometer suitable for aircraft measurement of background aerosol scattering coefficient. Atmos. Environ. 25, 2267–2276.

Carslaw, K.S., Clegg, S.L., Brimblecombe, P., 1995. A thermodynamic model of the system HCl–HNO_3–H_2SO_4–H_2O, including solubilities of HBr, from <200 K to 328 K. J. Phys. Chem. 99, 11557–11574.

Clegg, S.L., Brimblecombe, P., 2005. Comment on the "thermodynamic dissociation constant of the bisulfate ion from Raman and ion interaction modeling studies of aqueous sulfuric acid at low temperatures" by Knopf et al. J. Phys. Chem. A 109, 2703–2706.

Clegg, S.L., Brimblecombe, P., Wexler, A.S., 1998. A thermodynamic model of the system H^+–NH^{4+}–$SO4^{2-}$–NO^{3-}–H_2O at tropospheric temperatures. J. Phys. Chem. A 102, 2137–2154.

Davies, S.M., et al., 2010. Widespread dispersal of Icelandic tephra: how does the Eyjafjöll eruption of 2010 compare to past Icelandic events? J. Quart. Sci. 25, 605–611.

DeCarlo, P.F., Kimmel, J.R., Trimborn, A., Northway, M.J., Jayne, J.T., Aiken, A.C., Gonin, M., Fuhrer, K., Horvath, T., Docherty, K.S., Worsnop, D.R., Jimenez, J.L., 2006. Field-deployable, high-resolution, time-of-flight aerosol mass spectrometer. Anal. Chem. 78 (24), 8281–8289.

Flanagan, R.J., Kulmala, M., O'Dowd, C.D., 2011. Factors affecting in-cloud sulphate production in the marine environment. Atmos. Environ. minor revisions.

Flentje, H., Claude, H., Elste, T., Gilge, S., Köhler, U., Plass-Dülmer, C., Steinbrecht, W., Thomas, W., Werner, A., Fricke, W., 2010. The Eyjafjallajökull eruption in April 2010-detection of volcanic plume using in-situ measurements, ozonesondes and LIDAR-ceilometer profiles. Atmos. Chem. Phys. 10, 10085–10092.

Gassó, S., 2008. The impact of weak volcanic activity on marine clouds. J. Geophys. Res. doi:10.1029/2007JD009106.

Gysel, M., McFiggans, G.B., Coe, H., 2009. Inversion of tandem differential mobility analyser (TDMA) measurements. J. Aerosol Sci. 40, 134–151.

Heue, K.-P., Brenninkmeijer, C.A.M., Baker, A.K., Rauthe-Schöch, A., Walter, D., Wagner, T., Hörmann, C., Sihler, H., Dix, B., Frieß, U., Platt, U., Martinsson, B.G., van Velthoven, P.F.J., Hermann, M., Zahn, A., Ebinghaus, R., 2010. SO_2 and BrO observation in the plume of the Eyjafjallajökull volcano 2010: CARIBIC and GOME-2 retrievals. Atmos. Chem. Phys. Discuss. 10, 29631–29682.

Jayne, J.T., Leard, D.C., Zhang, X.F., Davidovits, P., Smith, K.A., Kolb, C.E., Worsnop, D.R., 2000. Development of an aerosol mass spectrometer for size and composition analysis of submicron particles. Aerosol Sci. Technol. 33 (1–2), 49–70.

Jennings, S.G., Kleefeld, C., O'Dowd, C.D., Junker, C., Spain, T. Gerard, O'Brien, P., Roddy, A.F., O'Connor, T.C., 2003. Mace Head Atmospheric Research Station – characterization of aerosol radiative parameters. Boreal Environ. Res. 8 (4), 303–314.

Jimenez, J.L., Jayne, J.T., Shi, Q., Kolb, C.E., Worsnop, D.R., Yourshaw, I., Seinfeld, J.H., Flagan, R.C., Zhang, X.F., Smith, K.A., Morris, J.W., Davidovits, P., 2003. Ambient aerosol sampling using the aerodyne aerosol mass spectrometer. J. Geophys. Res. 108 (D7) no.-8425.

Kleefeld, Ch., O'Dowd, C.D., O'Riely, S., Jennings, S.G., Aalto, P., Becker, E., Kunz, G., de Leeuw, G., 2002. The relative scattering of sub and super micron particles to aerosol light scattering in the marine boundary layer (MBL). J. Geophys. Res. 107. doi:10.1029/2000JD000262.

Klett, J.D., 1981. Stable analytical inversion solution for processing LIDAR returns. Appl. Opt. 20, 211–220.

Lance, S., Medina, J., Smith, J.N., Nenes, A., 2006. Mapping the operation of the DMT continuous flow, CCN counter. Aerosol Sci. Technol. 40, 1–13. doi:10.1080/02786820500543290.

Langmann, B., Varghese, S., Marmer, E., Vignati, E., Wilson, J., Stier, P., O'Dowd, C., 2008. Aerosol distribution over Europe: a model evaluation study with detailed aerosol microphysics. Atmos. Chem. Phys. 8, 1591–1607.

Langmann, B., Folch, A., Hensch, M., Matthias, V. Volcanic ash over Europe during the eruption of Eyjafjallajökull on Iceland, April–May 2010. Atmos. Environ., in this issue.

Martucci, M., Ovadnevaite, J., Ceburnis, D., Berresheim, H., Varghese, S., Martin, D., Flanagan, R., O'Dowd, C.D. Impact of volcanic ash plume aerosol on cloud microphysics. Atmos. Environ., in this issue.

Massucci, M., Clegg, S.L., Brimblecombe, P., 1999. Equilibrium partial pressures, thermodynamic properties of aqueous and solid phases, and Cl_2 production from aqueous HCl and HNO_3 and their mixtures. J. Phys. Chem. A 103, 4209–4226.

Nilsson, E., Swietlicki, E., Sjogren, S., Löndahl, J., Nyman, M., Svenningsson, B., 2009. Development of an H-TDMA for longterm unattended measurement of the hygroscopic properties of atmospheric aerosol particles. Atmos. Meas. Tech. 2, 313–318. doi:10.5194/amt-2-313-2009.

O'Connor, T.C., Jennings, S.G., O'Dowd, C.D., 2008. Highlights from 50 years of aerosol measurements at Mace Head. Atmos. Res. 90, 338–355. doi:10.1016/j.atmosres.2008.08.014.

O'Dowd, C., Varghese, S., Flanagan, R., Martin, D., Ceburnis, D., Ovadnevaite, J., Martucci, G., Bialek, J., Monahan, C., Berresheim, H., Vaishya, A., Grigas, T., Jennings, S.G., McVeigh, P., Moran, E., Lambkin, K., Semmler, T., McGrath, R. The Eyjafjallajökull ash plume – Part II, 2011, forecasting the plume dispersion. Atmos. Environ., in this issue.

Ovadnevaite, J., Ceburnis, D., Plauskaite-Sukiene, K., Modini, R., Dupuy, R., Rimselyte, I., Ramonet, M., Kvietkus, K., Ristovski, Z., Berresheim, H., O'Dowd, C.D., 2009. Volcanic sulphate and arctic dust plumes over the North Atlantic Ocean. Atmos. Environ. doi:10.1016/j.atmosenv.2009.07.007.

Pyle, D.M., 1999. Sizes of volcanic eruptions. In: Sigurdsson, H., et al. (Eds.), Encyclopedia of Volcanology. Academic Press, pp. 263–269.

Schumann, U., et al., 2011. Airborne observations of the Eyjafjalla volcano ash cloud over Europe during air space closure in April and May 2010. Atmos. Chem. Phys. 11, 2245–2279.

Varghese, S., Langmann, B., O'Dowd, C.D., 2011. Effect of horizontal resolution on meteorology and air-quality prediction with a regional scale model. Atmos. Res. doi:10.1016/j.atmosres.2011.02.007.

Vignati, E., Wilson, J., Stier, P., 2004. M7: an efficient size-resolved aerosol microphysics module for large-scale aerosol transport models. J. Geophys. Res. 109, D22202. doi:10.1029/2003JD004485.

von Glasow, R., 2010. Atmospheric chemistry in volcanic plumes. Proc. Natl. Acad. Sci. U. S. A. 107 (15), 6594–6599.

Wang, S.C., Flagan, R.C., 1990. Scanning electrical mobility spectrometer. Aerosol Sci. Technol. 13, 230–240. doi:10.1080/02786829008959441.

Yoon, Y.J., Ceburnis, D., Cavalli, F., Jourdan, O., Putaud, J.P., Facchini, M.C., Descari, S., Fuzzi, S., Jennings, S.G., O'Dowd, C.D., 2007. Seasonal characteristics of the physico-chemical properties of North Atlantic marine atmospheric aerosols. J. Geophys. Res. doi:10.1029/2005JD007044.

Yuan, T., Remer, L.A., Yu, H., 2011. Microphysical, macrophysical and radiative signatures of volcanic aerosols in trade wind cumulus observed by the A-Train. Atmos. Chem. Phys. Discuss. 11, 6415–6455. doi:10.5194/acpd-11-6415-2011.

Please cite this article in press as: O'Dowd, C., et al., The Eyjafjallajökull ash plume – Part I: Physical, chemical and optical characteristics, Atmospheric Environment (2011), doi:10.1016/j.atmosenv.2011.07.004